ELSEVIER

Applied Surface Science 111 (1997) 251–258

applied surface science

Secondary electron emission studies

A. Shih *, J. Yater, C. Hor, R. Abrams

Naval Research Laboratory, Washington, DC 20375, USA

Received 14 June 1996; revised 28 July 1996; accepted 23 August 1996

Abstract

Secondary-electron-emission processes under electron bombardment play an important role in the performance of a variety of electron devices. While in some devices, the anode and the grid require materials that suppress the secondary-electron-generation process, the crossed-field amplifier (CFA) is an example where the cathode requires an efficient secondary-electron-emission material. Secondary-electron-emission processes will be discussed by a three-step process: penetration of the primary electrons, transmission of the secondary electrons through the material, and final escape of the secondary electrons over the vacuum barrier. The transmission of the secondary electrons is one of the critical factors in determining the magnitude of the secondary-electron yield. The wide band-gap in an insulator prevents low-energy secondary electrons from losing energy through electron–electron collisions, thereby resulting in a large escape depth for the secondary electrons and a large secondary-electron yield. In general, insulating materials have high secondary-electron yields, but a provision to supply some level of electrical conductivity is necessary in order to replenish the electrons lost in the secondary-electron-emission process. Our secondary-emission study of diamond demonstrates that the vacuum barrier height can have a strong effect on the total yield. The combined effect of a large escape depth of the secondary electrons and a low vacuum-barrier height is responsible for the extraordinarily high secondary-electron yields observed on hydrogen-terminated diamond samples.

1. Introduction

Secondary-electron-emission processes under electron bombardment play an essential role in vacuum electronic devices. The materials used in the devices may need to be judiciously selected in some cases to enhance the secondary-electron emission and in other cases to suppress the emission. In microwave and millimeter wave power tubes, low secondary-electron-emission materials are desirable for depressed collectors in order to ensure a high efficiency in the energy conversion. Low-emission materials are also sought for coating the grids and the tube walls to prevent RF vacuum breakdown. On the other hand, high secondary-electron-emission materials are desirable for grids in electron multipliers and for cathodes in crossed-field devices, which is the area of our interest.

Crossed-field devices, e.g., magnetrons and crossed-field amplifiers (CFA), have established a long history of applications in radar systems. Their advantages include high efficiency, low cost, low voltage, and compactness. Consequently, they also find wide applications in microwave cooking, industrial processing, and radiation therapy equipment [1]. More recent applications are found in the generation of plasma for precision etching and in highly-efficient electric lighting. Exotic applications [1] are being explored for the generation of gigawatt-power

* Corresponding author. Fax: +1-202-7671280; e-mail address: shih@estd.nrl.navy.mil.

PII S0169-4332(96)00729-5

microwaves using a magnetically-insulated-line-oscillator (MILO) concept, and for beaming power (wireless power transmission) using an electronically-steerable-phased-array-module (ESPAM) concept. A good knowledge of secondary-electron-emission processes are crucial to the design of these devices. In some applications, e.g., AEGIS CFA's, only limited materials are available which have sufficiently high secondary-electron yields to satisfy the device's needs.

One of the major current challenges to crossed-field devices (CFD's) is noise reduction. The requirement on the signal-to-noise ratio becomes more stringent in radar applications, which demand high resolution and fast response for small and close-together targets in a cluttered environment. In microwave-oven applications, a potential interference with the neighboring band allocated to the new 'wireless' services calls for a reduction in the sideband noise of the magnetrons. At present, CFDs are much noisier than coupled-cavity traveling-wave tubes, although in principle they should have comparable noise characteristics [2,3]. Both experimental and theoretical efforts are pursuing noise reduction in CFDs with vigor. A thorough understanding of the secondary-electron-emission processes is essential to the success of these efforts. The secondary-electron-emission characteristics of the cathodes are found to have a major effect on the signal-to-noise ratio [4,5]. In particular, numerical simulations and experimental results have demonstrated that a very high electron emission (primary or secondary) would cause the transition of the CFD to a low noise state [5].

Secondary-electron-emission is a complex process, and theoretical treatments are numerous. Earlier treatments have been reviewed by Dekker [6] and by Hachenberg and Brauer [7]. More recent theoretical developments are summarized by Devooght et al. [8]. While the earlier models produced an overall agreement with experimental observations as good as the more elaborate later models, the main problem was the lack of justification for the simplifying assumptions [8]. These theories were able to predict most of the important characteristics of the secondary-electron emission, such as the secondary-electron yield as a function of primary-electron energy and the energy distribution of the secondary electrons. All of the theories predict well only the functional dependence (but not the magnitude) of the emission, except in the simple case of Al, which is close to the assumed free-electron picture [9]. We will discuss the secondary-electron-emission process in a mostly qualitative manner, as done by Jenkin and Trodden [10], and will support the discussion with our observations. The discussion of the secondary-emission process is organized according to the distinct steps used in all of the theories. The final step, which involves the overcome of the vacuum barrier, was considered to play only a minor role in the secondary-electron-emission process. However, the secondary-electron-emission behavior observed on diamond demonstrates the important role of the vacuum barrier.

2. Primary electron penetration and internal secondary electron generation

The theories treat secondary-electron emission as occurring in three distinct steps: (1) production of internal secondary electrons by kinetic impact of the primary electrons, (2) transport of the internal secondary electrons through the sample bulk toward the surface, and (3) escape of the electrons through the solid-vacuum interface.

The primary electrons are assumed to travel in a straight-ahead path, slowing down through collisions with electrons and ions and transferring kinetic energy to internally generated secondary electrons. Most of the theories treat the energy loss according to the 'power law',

$$-\frac{\mathrm{d}E}{\mathrm{d}x}=\frac{A}{E^n} \tag{1}$$

where E is the energy of a primary electron at a depth x, and A is an arbitrary constant. $N(x)$, the number of the secondary electrons produced in the layer $\mathrm{d}x$, is assumed to be equal to the energy loss in the layer $\mathrm{d}E$ divided by the average excitation energy B. Thus,

$$N(x)\mathrm{d}x=-\frac{\mathrm{d}E}{B} \tag{2}$$

A straight forward derivation [10] leads to

$$N(x)=\left(\frac{A}{2}\right)^{1/n+1}\frac{1}{B(R-x)^{n/n+1}} \tag{3}$$

and

$$R = \frac{E_0^{n+1}}{(n+1)A} \tag{4}$$

where R is the maximum penetration depth and E_0 is the initial energy of the primary electrons.

The best fit for the value of n was found to be 0.35, as determined by electron transmission measurements in Al_2O_3 [11] as well as by fitting the 'reduced yield curves' [6] taken from many materials. A quantum mechanical calculation [7] derived an approximate value of $n = 0.39$, which is fairly close to 0.35. The value obtained for n is valid over the energy range between 300 eV and 3 keV for the theory and 300 eV and 7 keV for the experiments.

Eq. (3) reveals the increasing importance of secondary-electron production near the end of the primary-electron path and Eq. (4) points out that the penetration depth of the primary electrons increases with increasing energy. The former fact is clearly shown in Fig. 1, which can be understood on a physical level by considering a simple description of the primary electrons moving through the solid. At high primary energies, the high-velocity electrons have a relatively short time to interact with the lattice electrons, and the internal yield per unit length is low. As the primary electrons lose energy, the interaction time increases and so does the yield. The combined effect is that as the primary-electron energy increases, the internal secondary electrons originate deeper beneath the surface.

The transport of secondary electrons through the material is modeled by either a single-scattering process or by a diffusion process which involves a large number of scattering events. Some later models explicitly take into account the electron-cascade process, which is the electron multiplication that occurs during the slowing-down of the internal secondary electrons. In all of the models, the escape of the internal secondary electrons is described by an exponential decay law with a characteristic escape depth X_s.

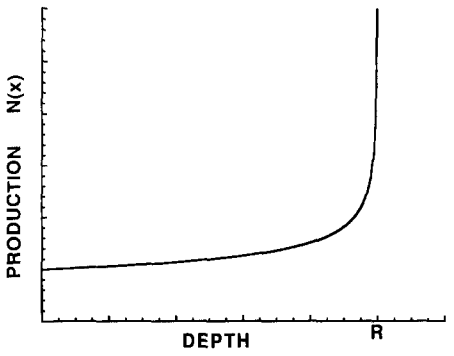

Fig. 1. The production rate of internal secondary electrons as a function of distance along the primary-electron path.

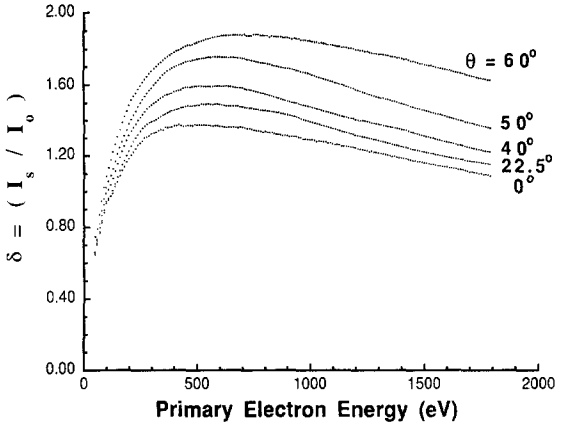

Fig. 2. Changes in the secondary-electron yield with incident angle θ. Normal incidence is at $\theta = 0°$. The data were taken on a clean molybdenum sample.

Based on the penetration-depth (R) and escape-depth (X_s) concepts, the shape of the secondary-electron yield curve as a function of the primary energy is easily explained [10]. At very low primary energies for which $R \ll X_s$, the internal secondary electrons escape efficiently, and due to the small primary energy only a few secondary electrons are created. Since the number of internal secondary electrons generated increases with primary energy, the observed yield also rises with primary energy. At very high primary energies for which $R \gg X_s$, the exponential nature of the escape process causes the decrease in the number of internal secondary electrons that escape to be more rapid than the increase in generation of internal secondary electrons. Consequently, the observed yield decreases with primary energy. The yield has a maximum value at a primary energy for which $R \approx X_s$. The resulting energy dependent yield curve is bell shaped, as commonly observed on most materials. An example is shown in Fig. 2 of yield curves taken on a molybdenum sample.

A similar qualitative discussion can be made about the variation in yield with incident angle. If the primary beam is incident at an angle θ to the surface, the maximum penetration depth is reduced by a factor $\cos\theta$ relative to that at normal incidence ($\theta = 0$), assuming a straight-ahead path for the primary beam. Consequently, the yields are larger at more oblique angles, and the enhancement in yield is more apparent at the higher primary energies for which $R \gg X_s$. The family of yield curves shown in Fig. 2 were taken at various θ on a clean molybdenum sample [12]. E_{max}, the energy at which the maximum yield occurs, increases with θ: E_{max} = 490, 520, 550, 580, and 660 eV for $\theta = 0$, 22.5, 40, 50, and 60°, respectively. Since E_{max} occurs at an energy for which $R\cos\theta \approx X_s$, a larger θ results in a larger R. Since the penetration depth R and the primary energy E are related by Eq. (4), a larger θ results in a larger E_{max} as well.

3. Transport of internal secondary electrons

In general, a primary electron with a reasonably high energy generates many internal secondary electrons. However, high secondary-electron yields are not always observed because most of the internal secondary electrons lose enough energy through collisions with electrons and ions to fall below the vacuum level. The energy-loss mechanisms for internal secondary electrons differ in metals and insulators. In metals, the secondary electrons lose energy by interacting with conduction electrons, lattice vibrations, and defects. The kinetic energy of a secondary electron must be at least $E_F + \phi$ when it reaches the surface in order to escape. E_F and ϕ are the Fermi energy and the work function of the metal, respectively, and the minimum escape energy $E_F + \phi$ is typically about 10 eV. This large minimum escape energy and the high collision probability due to the large number of conduction electrons result in the small secondary-electron yields found with metals. The maximum yield δ_{max} for a metal is on the order of unity, and it varies between 0.5 (for Li) and 1.8 (for Pt) [6].

In insulators, the minimum kinetic energy for a secondary electron to escape is the electron affinity χ, the difference between the vacuum level and the conduction-band minimum. The electron affinity is typically on the order of an electron volt for insulators. Since there are few conduction electrons in insulators, the secondary electrons lose energy through the excitation of valence electrons into the conduction band. The wide band gap prevents secondary electrons with kinetic energy less than E_{gap} from participating in such electron–electron collisions. For these electrons, electron–phonon and electron–impurity collisions are mainly responsible for the energy loss. Because of the absence of electron-electron scattering, the secondary electron loses much less energy as it moves through material and the escape depth becomes large. Therefore, in general, the yields are high in insulators [6]. For example, δ_{max} is 6.8 for NaCl and 25 for single-crystal MgO [6].

When the secondary-electron-yield coefficient exceeds one, the number of emitted secondary electrons exceeds the number of arriving primary electrons. Consequently, there is a net electron flow from the emitting sample into vacuum, and some level of electrical conductivity is necessary in the sample in order to replenish the lost electrons. Otherwise, sample charging will decrease the secondary emission yield to 1. Different approaches have been used in practice to provide electrical conductivity. In oxidized beryllium, only a top 10–20 Å thick layer is composed of BeO, beneath which metallic Be supplies the electrical conductivity. MgO/Au cermet is composed of a mixture of Mg and Au micro-crystal-

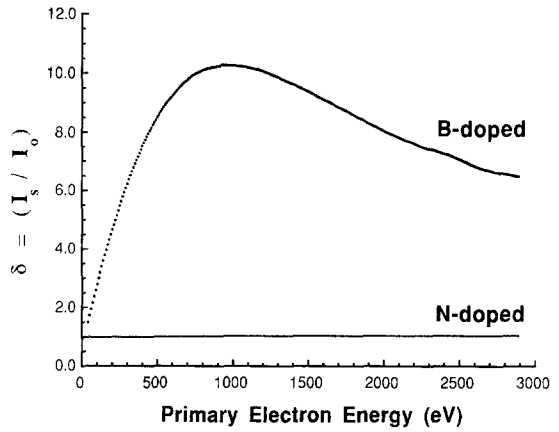

Fig. 3. Effect of electrical conductivity on the secondary-electron yield from diamond.

lites of about 50 Å diameter, with the Au particles providing the conducting path [13]. In diamond, appropriate dopants are used to provide the necessary electrical conductivity. Fig. 3 compares the secondary-electron-yield curves from N-doped and B-doped diamond samples. N is a deep donor in diamond, and at room temperature N-doped diamond samples are insulators. Fig. 3 shows that the secondary-electron yields from the N-doped diamond are very low. In contrast, B is a shallow acceptor in diamond, and therefore B-doped diamond samples are conductive. The three B-doped samples studied here have electrical resistivities between 50 Ω cm and 170 kΩ cm, and all three as-received samples showed comparably high yields. The yield curve taken from one of the samples is shown in Fig. 3.

4. Escape of secondary electrons over the vacuum barrier

Most of the theories do not explicitly treat the escape process at the solid-vacuum interface. A phenomenological approach by Bouchard and Carette [14] found that the potential barrier at a solid-vacuum interface controls the final shape of the secondary-electron energy distribution. This model and other theories do not regard the vacuum-barrier height as having a strong impact on the magnitude of the yield. For example, Jenkins and Trodden [10] argued that "most of the secondary electrons have energies greater than 10 eV. For this reason, we should expect that changes of the order of a volt in the work function of the surface would have only a small effect on the secondary emission coefficient". Furthermore, they provided experimental evidence of Na adsorption on W, which reduced the work function by nearly 3 eV but increased the yield by only 60%. However, the results of secondary-electron emission studies on diamond disagree with the conventional wisdom. We will show below that hydrogen-termination of diamond lowers the vacuum level by 1.45 eV but enhances the secondary-electron yield by more than an order of magnitude.

Recent investigations have found very high secondary-electron yields from hydrogen-terminated diamond samples [15–18]. Malta et al. [18] found a yield as high as 86 from a (100) diamond surface. Our study reveals that two of the key reasons for the extremely high secondary-electron yields from H-terminated diamond surfaces are: (1) the presence of a wide-band gap in diamond (5.47 eV) which allows low-energy secondary electrons to have large escape depths, and (2) a very low or even negative electron affinity at the surface which permits a large concentration of secondary electrons residing near the bottom of the conduction band to escape. These premises are supported by the analysis of the secondary-electron-yield data and the secondary-electron-energy-distribution spectra taken on diamond samples as presented below.

All of the diamond samples were grown by chemical vapor deposition (CVD) on Si substrates and then lifted off in a free-standing form. All samples were acid cleaned to remove surface impurities such as Si and non-diamond carbon. Most of the diamond samples that we studied were subjected to a 30-min hydrogenation process at 20 Torr hydrogen pressure, 600 W microwave power, and 800°C sample temperature. Hydrogenated diamond samples are H-terminated [19].

Fig. 4 shows an energy distribution curve (EDC) of the secondary electrons emitted from a H-terminated diamond sample. The measurement technique has been discussed in an earlier paper [20]. The energy of the secondary electrons is measured relative to the Fermi level E_F of the sample. The

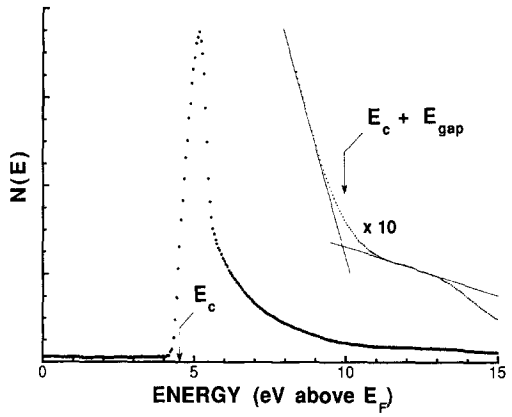

Fig. 4. Secondary-electron EDC of an as-received hydrogenated, B-doped, diamond sample. The data was taken at a primary electron energy of 1000 eV. The sharp peak is larger in spectra taken from samples with a saturated hydrogen coverage or in spectra taken with higher primary electron energies.

diamond sample used in the illustration is a B-doped sample, which has a Fermi level above but near the valence band maximum E_v. The conduction band minimum E_c is an energy E_{gap} above E_v, where E_{gap}, the band gap energy, is 5.47 eV for diamond. The position of E_c in Fig. 4 was determined by a method described previously by Shih et al. [21].

Photoemission EDCs from diamond have been shown to contain a high concentration of "quasi thermalized secondaries in the lowest conduction band" [22]. This high concentration of low-energy electrons is also present in the electron-stimulated secondary-electron distribution from diamond. They are called quasi-thermalized electrons because the energy width, although narrow (FWHM $\geq$ 0.5 eV), is much larger than that expected for fully thermalized electrons (0.025 eV). These electrons are piled up just above E_c as showed in Fig. 4. They represent a large fraction of the total emitted secondary electrons, and in some cases over 90% of the emitted electrons are contained in the sharp peak. When the vacuum level falls near or below E_c, these electrons can escape, resulting in a high secondary-electron yield. The vacuum level is ordinarily at the energy where the emission onset occurs, except in the case of a negative electron affinity (NEA) when the vacuum level can be below the emission onset energy. Fig. 4 shows that the emission onset occurs below E_c for the H-terminated diamond sample. This observation indicates the presence of a NEA on at least part of the surface.

H-termination of diamond is essential for the low electron affinity and is consequently crucial to the high secondary-electron yield. In Fig. 5, the secondary-electron EDC from a H-terminated diamond sample is compared with that from the same sample after heating at 1000°C for 15 min. The heating is sufficient to desorb a large fraction of the surface hydrogen. Accompanying the hydrogen desorption, the vacuum-barrier height increases by about 1.45 eV and is too high for the quasi-thermalized electrons to escape, resulting in a disappearance of the sharp peak in the EDC. Simultaneously, the secondary-electron yield drops precipitously. Fig. 6 shows the secondary-electron yield curves taken on the same sample before and after heating.

The other important factor for the large yield is the large escape depth of the low-energy secondary

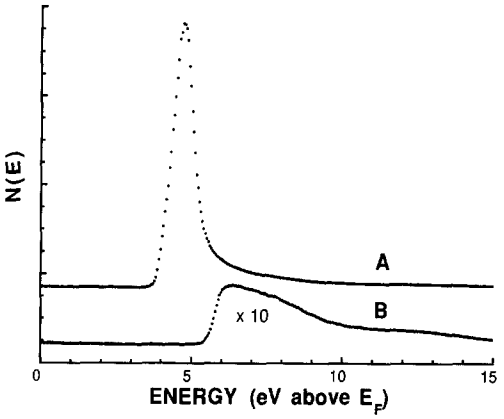

Fig. 5. Change in the secondary-electron EDC of a H-terminated, B-doped, diamond sample after a 1000°C heating. Curve A is the EDC taken from the H-terminated sample, and curve B is the EDC taken from the sample after the heating. The 1.45 eV rise in the vacuum level due to the heating prevents the high-concentration of low-energy secondary electrons from being emitted.

electrons because of the absence of electron–electron scattering. The 'turn-off' of electron–electron scattering is demonstrated in Fig. 4. In the enlarged part of the EDC, an abrupt change in the emission intensity occurs at the energy $E_c + E_{gap}$. Below $E_c + E_{gap}$, only electron–phonon and electron–impurity scatterings can occur, resulting in a large escape depth and relatively high emission intensities. Above $E_c + E_{gap}$, electron–electron scattering occurs which results in a small escape depth and a drop in the emission intensity.

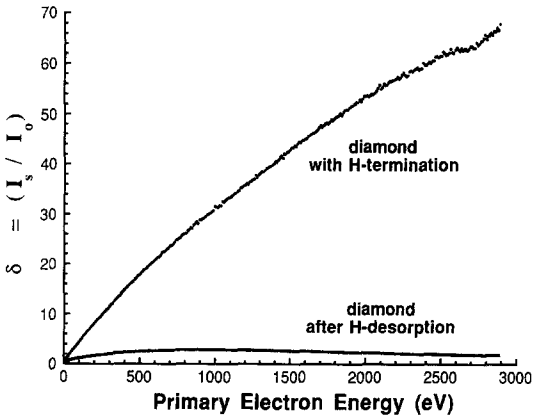

Fig. 6. A large reduction in the secondary-electron yield from diamond occurs with hydrogen desorption.

The quasi-thermalized electrons constitute a dominant portion of the secondary electrons emitted from H-terminated diamond samples. The low kinetic energy of these electrons may be responsible for the unusually large escape depth which is revealed by the unusually high E_{max}. Earlier we discussed that the maximum secondary-electron yield occurs at an energy for which $R \approx X_s$. A large X_s means a large R, which in turn means a high E_{max}. E_{max} occurs at about several hundred eV for most metals and at about 1000–2000 eV for most wide-band-gap materials [7]. For H-terminated diamond, the yield continues to rise over the 0 to 3000 eV energy range used in the measurements (see Fig. 6).

B impurities are introduced in the CVD diamond samples to provide the required electrical conductivity. Since electron–phonon and electron–impurity scatterings are the main energy-loss mechanisms for the low-energy secondary electrons, an excessively high impurity concentration may reduce the escape depth and the yield. Fig. 7 compares the yield curves taken on diamond samples with different B-doping levels. The higher yield curves are typical for low or moderately B-doped diamond samples which have a resistivity between 50–170 kΩ cm and are transparent. The lower yield curve is taken from the highly B-doped sample which appears black and opaque and has a resistivity between 50–170 Ω cm. We have not studied any sample with a resistivity between 170 Ω cm and 50 kΩ cm.

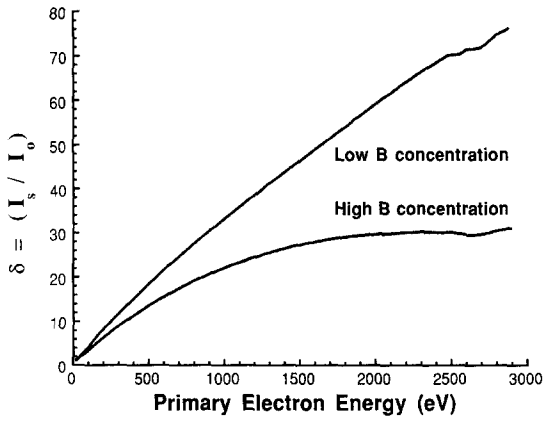

Fig. 7. Effect of the B impurity level on the secondary-electron yield from diamond.

5. Summary

Secondary-electron-emission processes have been discussed using a three-step process: (1) generation of internal secondary electrons during the slow-down of primary electrons, (2) transport of the internal secondary electrons through the material, and (3) the final escape of the electrons over the vacuum barrier. A consideration of the penetration depth of the primary electrons and its relation to the escape depth of the internal secondary electrons explains the dependence of the secondary-electron yield on the energy and the incident angle of the primary electrons. An examination of the scattering events experienced by the internal secondary electrons explains the difference in yield found for a metal and an insulator. The presence of a wide band gap allows a large escape depth for the low-energy secondary electrons, but it also depletes the number of conduction electrons available to sustain the emission process. Examples of measures employed to supply electrical conductivity were given.

Diamond provides an opportunity to explore a possible novel secondary-electron-emission process; the novel characteristics are manifested by the distinctive sharp feature in the secondary-electron EDC and by the exceedingly high yields. The final step, which involves the overcome of the vacuum barrier, was previously considered to play only a minor role in the secondary-emission process. However, a high concentration of quasi-thermalized secondary electrons is present above the conduction-band minimum of diamond. Hydrogen-termination on diamond surfaces lowers the vacuum barrier height to near or below the conduction-band minimum which releases a flood of low-energy secondary electrons and boosts the total yield tremendously. The low electron affinity at the surface and the large escape depth of the secondary electrons are responsible for the extraordinarily high secondary-electron yields from H-terminated diamond samples.

The potentially rapid degradation in the yield from H-terminated diamond due to electron and ion impingement prevents the wide application of diamond in actual devices [16]. However, the knowledge gained from the secondary emission study of diamond points to the possibility of using other high

secondary-yield materials, namely wide band-gap materials with low electron affinities.

Acknowledgements

The diamond samples studied were supplied by Drs. P. Pehrsson and J. Butler of the NRL Chemistry division. This work is supported in part by NSWC/Crane Division and in part by the Vacuum Electronics Initiative.

References

[1] D. Chernin and Y.Y. Lau, ed., Proc. of the First Int. Workshop on Crossed-Field Devices, August 15–16, 1995, Ann Arbor, Michigan.
[2] T.E. Ruden, G.E. Dombroski, D. Hobbs and G. Boles, Proc. of the First Int. Workshop on Crossed-Field Devices (1995) 66.
[3] G. Ya. Levin, L.A. Semenov, A. Ya Usikov, Yu.A. Belov, Sov. J. Comm. Tech. Elect. 37 (1992) 128.
[4] J.Z. Ye, R. MacGregor, C. Chan and T.E. Ruden, Proc. of the First Int. Workshop on Crossed-Field Devices (1995) 202.
[5] H.L. McDowell, Proc. of the First Int. Workshop on Crossed-Field Devices (1995) 236.
[6] A.J. Dekker, in: Solid State Physics, Advances in Research and Applications, eds. F. Seitz and D. Turnbull (Academic Press, New York, 1958) p. 251.
[7] O. Hachenberg and W. Brauer, in: ed. L. Marton, Advances in Electronics and Electron Physics (Academic Press, New York, 1959) p. 413.
[8] J. Devooght, A. Dubus and J.C. Dehaes, Phys. Rev. B 36 (1987) 5093.
[9] A. Dubus, J. Devooght and J.C. Dehaes, Phys. Rev. B 36 (1987) 5110.
[10] R.O. Jenkins and W.G. Trodden, Electron and Ion Emission (Dover, New York, 1965) p. 54.
[11] J.R. Young, Phys. Rev 103 (1956) 292.
[12] A. Shih and C. Hor, IEEE Trans. Elect. Devices 40 (1993) 824.
[13] V.H. Ritz, A. Shih and B. Sobocinski, Surf. Interface Anal. 18 (1992) 514.
[14] C. Bouchard and J.D. Carette, Surf. Sci. 100 (1980) 251.
[15] G.T. Mearini, I.L. Krainsky, Y.X. Wang, J.A. Dayton, Jr., R. Ramesham and M.F. Rose, Thin Solid Films 253 (1994) 151.
[16] G.T. Mearini, I.L. Krainsky and J.A. Dayton, Jr., Surf. Int. Anal. 21 (1994) 138.
[17] D.P. Malta, J.B. Posthill, T.P. Humphreys, R.E. Thomas, G.G. Fountain, R.A. Rudder, G.C. Hudson, M.J. Mantini and R.J. Markunas, Mat. Res. Soc. Symp. Proc. 339 (1994) 39.
[18] D.P. Malta, J.B. Posthill, T.P. Humphreys, M.J. Mantini and R.J. Markunas, Mat. Res. Soc. Symp. Proc. 416 (1996) 311.
[19] B.D.Thoms, P.E. Pehrsson and J.E. Butler, J. Appl. Phys. 75 (3) 1804 (1994).
[20] A. Shih, J. Yater, C. Hor and R. Abrams, IEEE Trans. Elect. Devices 41 (1994) 2448.
[21] A. Shih, J. Yater, P. Pehrsson, J. Butler, C. Hor and R. Abrams, Mat. Res. Soc. Symp. Proc. 416 (1996) 461.
[22] F.J. Himpsel, J.A. Knapp, J.A. Van Vechten and D.E. Eastman, Phys. Rev. B 20 (2) (1979) 624.